Journal of Thermal Analysis and Calorimetry, Vol. 69 (2002) 65–75

SCANDIUM DIPIVALOYL METHANATE AS A VOLATILE PRECURSOR FOR THIN FILM DEPOSITION
Coupling of mass spectrometer to thermobalance

K. Mészáros-Szécsényi[1,2], *J. Päiväsaari*[1], *M. Putkonen*[1], *L. Niinistö*[1*] *and G. Pokol*[3]

[1]Laboratory of Inorganic and Analytical Chemistry, Helsinki University of Technology, P.O. Box 6100, FIN-02015 Espoo, Finland
[2]Permanent address: University of Novi Sad, Faculty of Sciences, Institute of Chemistry, YU-21000 Novi Sad, Trg. Dositeja Obradovica 3, Yugoslavia
[3]Institute of General and Analytical Chemistry, Budapest University of Technology and Economics, H-1521 Budapest, Hungary

Abstract

The coupling of a quadrupole mass spectrometer (QMS) via a heated capillary to a commercial thermogravimetric analyser is described. The amu and temperature ranges available were up to 1000 amu and 1500°C, respectively. The system was evaluated with test compounds, yielding gaseous species in the *m/z* range of 17–80, and then used for the study of thermal behaviour of scandium dipivaloyl methanate or $Sc(thd)_3$ which is discussed in detail. $Sc(thd)_2$ appears as the major Sc-containing species with *m/z*=411 in the gas phase at 200–300°C.

Keywords: ALD, CVD, Sc precursor, TG-MS, thin films

Introduction

Combining mass spectrometry simultaneously with thermogravimetry significantly increases the information content of a thermoanalytical run and enhances the possibilities to correctly interpret the mechanism of thermal decomposition reactions. The information obtainable from a combined TG-MS run can also be used to evaluate precursors and processes for the growth of thin films by chemical vapour deposition (CVD) and atomic layer deposition (ALD) methods. For a better understanding and control of a CVD or ALD process it is necessary to know, besides the thermal stability of the precursor, also the composition of the vapour phase. To solve this kind of problem, *i.e.* to carry out an evolved gas analysis (EGA), mass spectrometry has proven to be a very powerful tool.

Due to its superiority over most other EGA methods, mass spectrometry has established itself over the past 30 years or so as the method of choice for monitoring of gaseous species evolved in a thermoanalytical process (TG or DTA). The coupled TG-MS methods have been frequently reviewed [1–5] and several TG-MS interface

1418–2874/2002/ $ 5.00
Akadémiai Kiadó, Budapest

constructions have been described. The interface constructions are most often based on a heated capillary to reduce the pressure and to transport the gaseous sample [6, 7]. Other interface solutions for a simultaneous EGA, *i.e.* coupling of a TA instrument to a gas analyser, have been presented as well. They involve a single- or double-step coupling to a MS instrument through orifice [8], jet separator [9] or skimmer system [10]. We have earlier described the coupling of a quadrupole MS (QMS) to a thermogravimetric analyser via a heated capillary [7]. There are also commercially available coupled TG-MS instruments. On the other hand, a more versatile solution is to tailor a connection mode between available MS and TG instruments as we did earlier in the case of Perkin Elmer TGA 7 and Leybold–Heraeus IQ 200 quadrupole mass spectrometer [7]. In this paper we describe a connection mode between Hiden QMS and Seiko TG-DTA analyser through a heated capillary interface. The performance of the instrument was tested with three test substances, *viz.* $CaC_2O_4 \cdot H_2O$, $CuSO_4 \cdot 5H_2O$ and $Fe(NH_4)(SO_4)_2 \cdot 12H_2O$. The system was then used to study the thermal decomposition of scandium dipivaloyl methanate, $Sc(thd)_3$ (dipivaloyl methanate or *thd* = 2,2,6,6-tetramethyl-3,5-heptanedionate).

Scandium dipivaloyl methanate, $Sc(thd)_3$ belongs to the metal β-diketonates. These compounds are often used as precursors for thin film deposition by CVD and ALD methods because of their volatility and relatively high thermal stability in the vapour phase [11]. The mass spectra of several rare earth β-diketonates have been reported in literature, including those of $Y(thd)_3$ [12], $Ce(thd)_4$ [13, 14] and $Gd(thd)_3$ [15].

In this work, we present a TG-MS study of $Sc(thd)_3$, which has been used as a precursor for atomic layer deposition [16, 17]; the results of the ALD growth of Sc_2O_3 thin films have been reported elsewhere [18]. Recently, Sc_2O_3 thin films from a $Sc(thd)_3$ precursor have also been deposited by CVD [19]. Also the integration of a QMS instrument into an ALD reactor has been described and used for *in situ* analysis of the gas phase during the deposition process [20, 21].

Experimental

Thermoanalytical measurements were carried out using a Seiko simultaneous TG-DTA 320 instrument while the simultaneous EGA measurements were performed by means of a QMS instrument of Hiden Analytical Ltd, type HAL-1001 with mass range up to 1000 amu.

$Sc(thd)_3$ (CAS 15492-49-6, M=594.77 g mol^{-1}) was synthesised with the method presented in literature [22]. As a first step, $Sc(NO_3)_3 \cdot xH_2O$ was prepared from 2 g of Sc_2O_3, which was dissolved in 6.1 cm^3 nitric acid (65 mass%). After the evaporation of the solution, 10 g of $Sc(NO_3)_3 \cdot xH_2O$ crystals were obtained. $Sc(NO_3)_3 \cdot xH_2O$ was vacuum-dried at 50°C. The number of water molecules, i.e. the value of x, was verified to be 4.6 by means of thermogravimetry. Then 10.3 cm^3 of H(thd) was dissolved in 30 cm^3 of 96 vol% ethanol (Etax A, Primalco) in a round-bottomed flask. The solution was continuously stirred. Next, 2 g of NaOH pellets dissolved in 50 cm^3 of 50 vol% ethanol were slowly added. Finally, 5.3 g of $Sc(NO_3)_3 \cdot 4.6\ H_2O$ dissolved in 50 cm^3 of 50 vol% ethanol

was added slowly. Solution turned into white as $Sc(thd)_3$ was formed. After about one hour of stirring the mixture was distilled under vacuum. $Sc(thd)_3$ was separated by vacuum filtration, dried in vacuum at 50°C and purified by sublimation at 110°C. Yield after sublimation was 9.1 g (91%). The purity and volatility of the product were verified by FTIR and thermogravimetry in vacuum, respectively.

Coupling the mass spectrometer to the thermobalance

In contrast to Perkin Elmer TGA 7 [7], the Seiko TG-DTA 320 instrument is a horizontal thermobalance with a horizontal gas-flow outlet. This outlet was employed for the coupling of the QMS through a pressure reducing heated silica capillary interface. Sampling into capillary ($\varnothing_i$=0.32 mm, length=2 m) was from the atmospheric pressure inside the TA instrument. The temperature of the resistively heated capillary was adjusted to approximately 150°C by changing the current. The ceramic outlet tube of the thermobalance was fitted into the capillary through a connecting metal tube, which was fitting well the outlet in order to keep the capillary assembly fixed. The tube was connected to the heated capillary line and it reached the inside of the balance near to the sample holder. The end of the tube, which was fixed to the sampling line, contained holes for the purge gas outlet (Fig. 1). Through the metal tube placed near to the sample holder a representative sample could be obtained for the MS measurement without any time lag between the decomposition and the detection. Actually, because of the greater sensitivity of the MS detection compared with the sensitivity of the balance, no time-lag was observed between the TG (DTG, DTA)- and MS-signals.

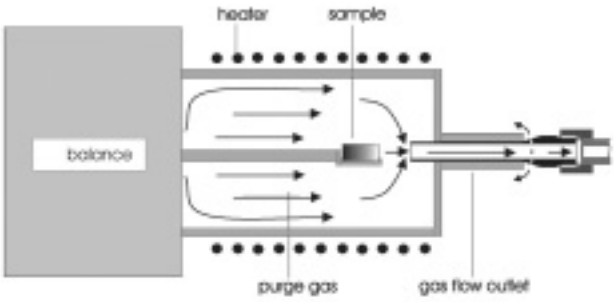

Fig. 1 The connection between the coupled thermobalance and QMS through a heated capillary

The Seiko instrument is a thermobalance controlled by a built-in computer, while the QMS was controlled by PC and MASsoft (Ver. 3.5.3.) software developed by Hiden Analytical Ltd. Both instruments could send their output signals to a common plotter and the results could be assessed by overlaying the corresponding time range curves. It was also possible to transfer data to a data analyser programme like Origin and evaluate the results after the measurement. The block diagram of the coupled instruments is presented in Fig. 2.

This configuration gave the expected, satisfactory results with the test samples ($CaC_2O_4 \cdot H_2O$, $CuSO_4 \cdot 5H_2O$ and $Fe(NH_4)(SO_4)_2 \cdot 12\ H_2O$) the decomposition products

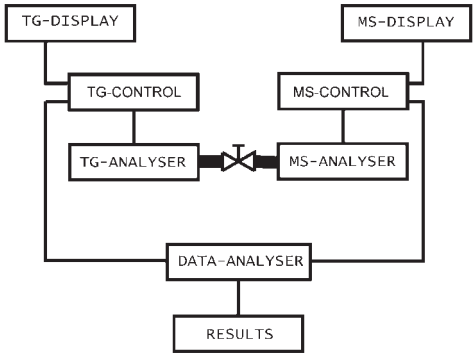

Fig. 2 A block diagram of the configuration used in the simultaneous TG-MS measurements

of which are gases or highly volatile compounds with molecular masses ranging from 17 to 80 (NH_3, H_2O, CO, CO_2, SO_2, SO_3). However, for the detection of the decomposition products with low volatility, an outside thermal isolation of the gas-flow outlet, consisting of a metal tube and unheated part of the capillary, is necessary. In addition, the metal tube reaching the inside of the furnace improves the heat transfer around the capillary tip outside of the heated transfer line. With this isolation the thermal stability of the fused silica capillary and the limited capillary heating temperature determine the limits of the MS sampling.

Results and discussion

Thermal decomposition of the scandium dipivaloyl methanate

With the equipment described above, $Sc(thd)_3$ decomposition was studied with heating rates of 5 and 10°C min^{-1} both in air and argon atmospheres. The sample mass ranged from 5 to 25 mg, a typical value being 8 mg. Aluminium oxide crucibles were employed with aluminium oxide as DTA reference material.

The thermal decomposition curves of the title compound, recorded with 5 and 10°C min^{-1} heating rates in an argon atmosphere, are presented in Fig. 3. Essentially similar decomposition curves are obtained in air. DTA curve shows a phase transition at 123°C onset temperature and at 153°C the melting of the sample is observed. According to the TG curve the evaporation and the thermal decomposition of the compound is a single-step process which is completed in a temperature range of approximately 160–320°C, depending on the sample mass. For the typical sample mass of about 8 mg the decomposition range was 165–265°C. The evolving of gaseous decomposition products during the evaporation was monitored by the QMS assembly described above.

MS fragmentation of the sample was followed in the 50–130, 350–420 and 530–600 amu ranges over a dynamic temperature interval of 20–350°C using 70 eV ionisation potential and emission current of 1000 μA. The mass spectra of the $Sc(thd)_3$ at maximum peak intensities are shown in Fig. 4., while the ionic pressure intensities detected with secondary electron multiplier (SEM) in the mass spectra at different temperatures are listed in Table 1.

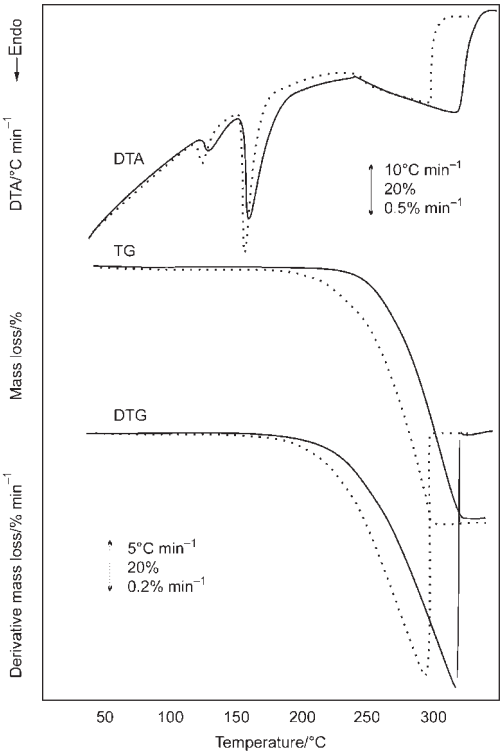

Fig. 3 Thermal decomposition curves of $Sc(thd)_3$ recorded with heating rates 5 (dashed line) and 10°C min^{-1} (solid line) in an Ar-atmosphere

Table 1 Ionic pressure intensities (i) produced by $Sc(thd)_3$ at different temperatures

	Temperature/°C					
	≈200		>250		>300	
m/z fragment	$i\cdot10^{11}$/torr	i/i_{max}/%	$i\cdot10^{11}$/torr	i/i_{max}/%	$i\cdot10^{11}$/torr	i/i_{max}/%
594 $Sc(thd)_3^+$	–	–	–	–	0.1	0.2
537 $[Sc(thd)_3–C_4H_9]^+$	–	–	0.5	1.0	1.2	2.7
411 $Sc(thd)_2^+$	0.05	3.0	1.0	30.0	4.5	10.0
396 $[Sc(thd)_2–CH_3]^+$	–	–	0.1	2.0	0.3	0.7
381 $[Sc(thd)_2–2CH_3]^+$	–	–	0.05	1.0	0.2	0.4
354 $[Sc(thd)_2–C_4H_9]^+$	–	–	0.1	2.0	0.5	1.1
127 $[(thd)–C_4H_8]^+$	1.00	67.0	1.7	51.0	3.5	7.8
126 $[(thd)–C_4H_9]^+$	0.70	47.0	0.7	21.0	0.70	1.5
57 $C_4H_9^+$	1.50	100.0	3.0	91.0	10.0	22.0
56 $C_4H_8^+$	1.50	100.0	3.3	100.0	45.5	100.0

As data in Table 1 show, the intensity of all fragments increases with temperature, indicating an increasing decomposition of the sample at higher temperatures. The peaks with highest intensity belong to the $Sc(thd)_2^+$, $[Sc(thd)_3–C_4H_9]^+$, $Sc(thd)_3^+$ molecular fragments and to the fragments of the ligand. Besides these, fragments with composition of $[Sc(thd)_2–CH_3]^+$, $[Sc(thd)_2–2CH_3]^+$, and $[Sc(thd)_2–C_4H_9]^+$ were detected.

In the beginning of the decomposition only the fragments of the $Sc(thd)_2^+$ and the ligand peaks were detected with significant intensity [23]. Peaks with *m/z* ratio of 56 ($C_4H_8^+$) and 57 amu ($C_4H_9^+$) appeared with the same intensities. Fragments of $C_7H_{10}O_2^+$ and $C_7H_{11}O_2^+$ were also present in the spectra with approximately same intensities. Ionic current due to the other fragments was negligible at this stage of the decomposition. With increasing temperature all peak intensities increased but at the same time the intensity ratio also changed: the ionic current of the $C_4H_9^+$ fragment decreased while the intensity of the $C_4H_8^+$ fragment increased together with the intensity of the $C_7H_{11}O_2^+$ fragment. Above 250°C all peaks listed were present with significant intensities.

The highest peak of the spectra at all temperatures belonged to the $C_4H_8^+$ fragment. When comparing the intensity of this peak with the intensity ratio of the other peaks, it was noted that it changed with temperature indicating probably a different thermal decomposition mechanism. On the basis of these data, we assume that the decomposition proceeds through the following stages:

1. At lower temperatures mainly dissociation of one ligand takes place:

$$Sc(thd)_{3(g)} \rightarrow Sc(thd)_{2(g)}+thd_{(g)} \quad (1)$$

The thd radical formed decomposes immediately, partly through a McLafferty rearrangement.

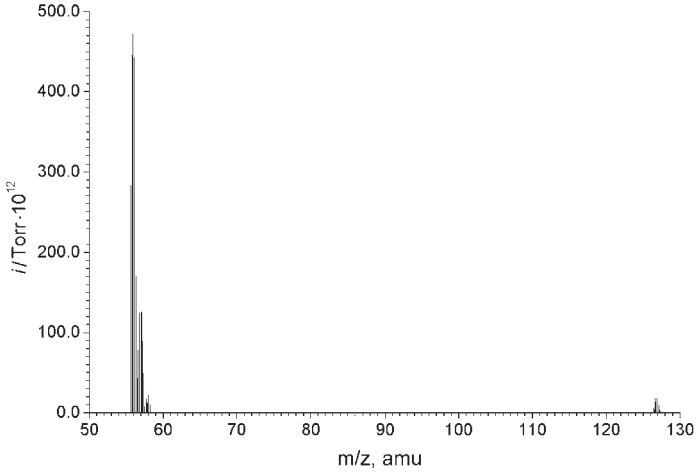

Fig. 4a Mass spectra of $Sc(thd)_3$ at maximum peak intensities in the 50–130 amu range

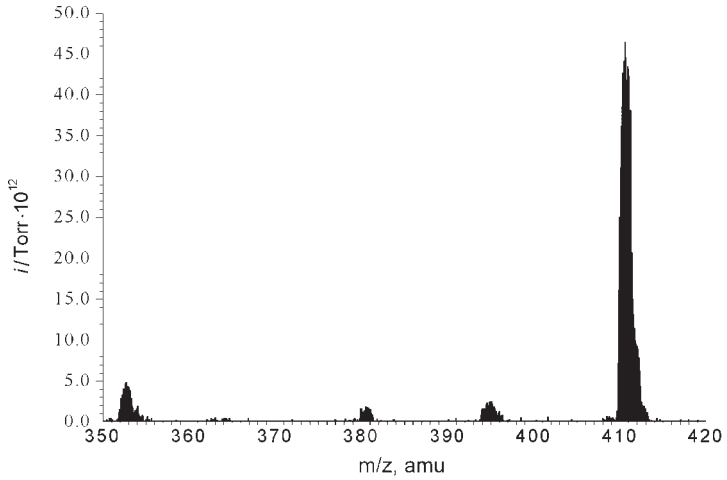

Fig. 4b Mass spectra of $Sc(thd)_3$ at maximum peak intensities in the 350–420 amu range

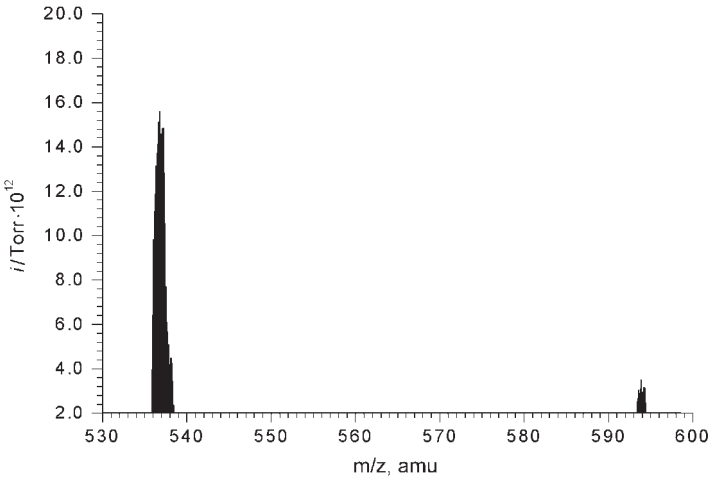

Fig. 4c Mass spectra of $Sc(thd)_3$ at maximum peak intensities in the 530–600 amu range

2. With an increasing temperature the decomposition of the $C_7H_{11}O_2^+$ and $C_7H_{10}O_2^+$ fragments also increases which is seen as a sharp rise of the intensities of the $C_4H_8^+$ and $C_4H_9^+$ fragments.

In contrast to the fragmentation of the $Y(thd)_3$ complex, where at lower temperatures the peak with highest intensity belongs to the $[Y(thd)_3–C_4H_9]^+$ fragment [12], the corresponding $Sc(thd)_3$ compound produces the $[Sc(thd)_3–C_4H_9]^+$ peak at higher temperatures with a significantly lower relative intensity. As the *terc*butyl-group is an electron donor group, it transfers some of its electrons to the chelate ring, weakening this way the $C–C(CH_3)_3$ bond. However, this transfer is less obvious in the $Sc(thd)_3$, resulting in the cleavage of the *terc*-butyl-group at higher temperatures.

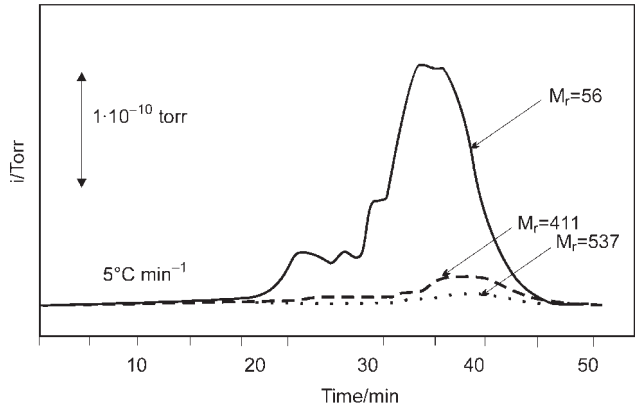

Fig. 5 Peak intensities of the fragments *m/z*=56, 411 and 537 amu as a function of time

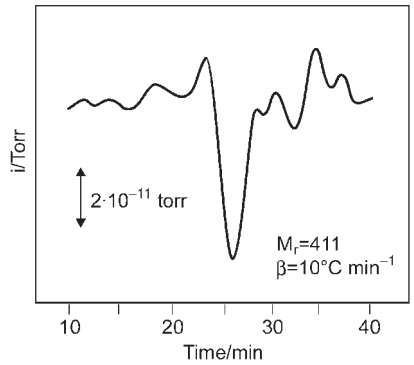

Fig. 6 Shape of the MS-peak of the $Sc(tdh)_2^+$ (*m/z*=411 amu) fragment after repeated measurements in the same capillary showing the signs of retention (tailing)

Thus, the proportion of the $[Sc(thd)_3–C_4H_9]^+$ fragment increases with increasing temperature while the relative intensities of the other peaks decrease:

$$Sc(thd)_3 \rightarrow [Sc(thd)_3–C_4H_9]+C_4H_9 \quad (2)$$

At higher temperatures the McLafferty's rearrangement of the ligand seems to be preferred over simple fragmentation; above 300°C the $C_4H_9^+$ fragment probably belongs to the broken off *terc*-butyl-groups. Under dynamic conditions it is likely that both processes proceed simultaneously.

Besides the different decomposition pattern, the overall thermal stability of the $Sc(thd)_3$ complex is significantly higher than the stability of the corresponding yttrium compound. This is a consequence of the greater bond strength between the ligand donor atoms and scandium ion, mainly due to the higher charge/radius ratio as compared to that of yttrium.

In principle, all the fragments can be monitored during the decomposition process on a temperature (time) scale (Fig. 5). The most easily followed fragment is that with the

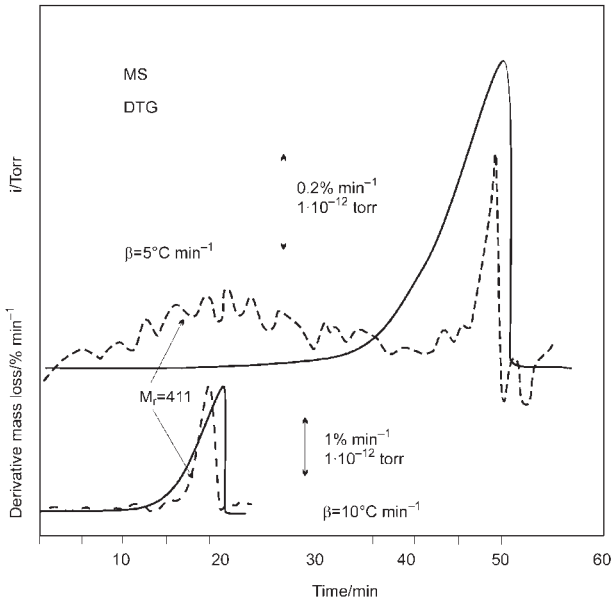

Fig. 7 Combined MS and DTG curves recorded for the $Sc(tdh)_2^+$ fragment originating from the $Sc(thd)_3$ sample

highest ionic current intensity which in this case belongs to the fragment with 56 amu. However, this peak is not specific for the present compound alone, but is typical for all Ar–*n*-C_5H_{11}, Ar–*iso*-C_5H_{11}, ArO–*n*-C_4H_9, ArO–*iso*-C_4H_9 compounds, pentyl ketone, *etc.* Out of the many compound-characteristic peaks, the $Sc(thd)_2^+$ peak (411 amu) appears suitable for continuous monitoring. However, the retention of the this fragment, being coordinatively unsaturarated, is sometimes high, especially when the measurement is repeated with the same capillary, as can be seen in Fig. 6. On the other hand, there is no significant retention of the smaller 56 amu fragment. The combined DTG-MS curves at 5 and 10°C min^{-1} heating rates are presented in Fig. 7.

Conclusions

The Hiden QMS is a universal MS instrument. In order to make a full-scale use of it, the connection adapter for every specific purpose should be easily commutable. In this case it is achieved by unscrewing the metal tube; the QMS is then ready for adaptation to other instruments, e.g., to the ALD reactor.

The TG-MS measurements of the test samples with a heated capillary to 150°C were easily conducted and without condensation. However, difficulties arose during the measurement of a compound yielding less volatile decomposition products. At 150°C the capillary was clogged by condensation. Therefore an increase of the capillary temperature up to 180°C was applied. Even at this temperature the retention of the sample was observed. Only with long empty runs and degassing we could get rid

of the retained compound. Significant peak broadening was observed with high sample masses and low purge gas flow rate especially in experiments with low heating rate. With a clean capillary, a lower sample mass and an optimal purge gas flow, however, well resolved mass spectra can be obtained which provide very valuable data for the interpretation of the decomposition mechanism. The sharp MS-peak – time curves can be easily related to the thermal decomposition (TG-DTG) curves. Compared with our previous system also based on a TG-QMS coupling [7], the present one has a significantly wider mass range and higher sensitivity, meaning smaller samples. An integration of MS data to a thermogram to produce a practical and informative plotter output would require some additional programming work, however.

TG-MS data reveal that when $Sc(thd)_3$ is heated, $Sc(thd)_2$ appears as a major Sc-containing species in the gas phase. $Sc(thd)_2$ being volatile, sufficiently stable and coordinatively unsaturated is probably responsible for the Sc_2O_3 thin film growth from the $Sc(thd)_3$ precursor in the recently developed ALD/ALE process [18]. The relatively small size of the $Sc(thd)_2$ species makes it an attractive choice for special applications such as conformal coating of edges and even pores, which is an emerging application of ALD [24, 25].

* * *

One of us (K.M.Sz.) wishes to acknowledge scholarship for a research stay at HUT from the Finnish Center for International Mobility (CIMO). The support of CIMO for shorter research visits between HUT and BUTE for L. N., J. P. and G. P. is acknowledged as well. The authors wish also to thank Ms. Minna Nieminen (M. Sc.) for the synthesis of the Sc precursor.

References

1 W. R. Holdiness, Thermochim. Acta, 75 (1984) 361.
2 D. Dollimore, G. A. Gamlen and T. J. Taylor, Thermochim. Acta, 75 (1984) 59.
3 E. Kaisersberger and E. Post, Thermochim. Acta, 295 (1997) 73.
4 J. P. Redfern, Polymer Intl., 26 (1991) 51.
5 H. G. Langer, In: I. M. Kolthoff and P. J. Elving (Eds.), Treatise on Analytical Chemistry, Vol. 12., Interscience, New York 1982, p. 229.
6 E. Kaisersberger and W.-D. Emmerich, Thermochim. Acta, 85 (1985) 275.
7 T. Leskelä, M. Lippmaa, L. Niinistö and P. Soininen, Thermochim. Acta, 214 (1993) 9.
8 A. R. McGhie, Thermochim. Acta, 234 (1994) 21.
9 E. Clarke, Thermochim. Acta, 51 (1981) 7.
10 T. Arii and Y. Masuda, Thermochim. Acta, 342 (1999) 139.
11 M. Tiitta and L. Niinistö, Chem. Vap. Deposition, 3 (1997) 167.
12 G. V. Girichev, N. I. Giricheva, N. V. Belova, A. R. Kaul', N. P. Kuz'mina and Yu. Gorbenko, Russ. J. Inorg. Chem. (Engl. transl.), 38 (1993) 320.
13 M. Leskelä, R. Sillanpää, L. Niinistö and M. Tiitta, Acta Chem. Scand., 45 (1991) 1006.
14 T. Leskelä, K. Vasama, G. Härkönen, P. Sarkio and M. Lounasmaa, Adv. Mater. Opt. Electron., 6 (1996) 169.
15 C. Hirayama, R. G. Charles, R. D. Straw and P. G. Sullivan, Thermochim. Acta, 88 (1985) 407.

16 T. Suntola, In: D. A. Glocker (Ed.), Handbook of thin film process technology, IOP Publishing Ltd., London 1995, p. B1.5:1.
17 L. Niinistö, Proc. Int. Semicond. Conf. CAS, 1 (2000) 33.
18 M. Putkonen, M. Nieminen, J. Niinistö and L. Niinistö, Chem. Mater, 3 (2001) 4701.
19 K. A. Fleeting, H. O. Davies, A. C. Jones, P. O'Brien, T. J. Leedham, M. J. Crosbie, P. J. Wright and D. J. Williams, Chem. Vap. Deposition, 5 (1999) 261.
20 M. Ritala, M. Juppo, K. Kukli, A. Rahtu and M. Leskelä, J. Phys. IV France, 9 (1999) 1021.
21 M. Juppo, A. Rahtu, M. Ritala and M. Leskelä, Langmuir, 16 (2000) 4034.
22 K. J. Eisentraut and R. E. Sievers, J. Inorg. Nucl. Chem., 29 (1967) 1931.
23 http://webbook.nist.gov/chemistry, 24.7.2001.
24 C. Dücsö, N. Q. Khanh, Z. Horváth, I. Bársony, M. Utriainen, S. Lehto, M. Nieminen and L. Niinistö, J. Electrochem. Soc., 143 (1996) 683.
25 M. Utriainen, S. Lehto, L. Niinistö, C. Dücsö, N. Q. Khanh, Z. Horváth, I. Bársony and B. Pécz, Thin Solid Films, 297 (1997) 39.